Title
Mitf regulates osteoclastogenesis by modulating NFATc1 activity

Journal
Experimental Cell Research, 328(1)

ISSN
0014-4827

Authors
Lu, Ssu-Yi
Li, Mengtao
Lin, Yi-Ling

Publication Date
2014-10-01

DOI
10.1016/j.yexcr.2014.08.018

Peer reviewed

Published in final edited form as:
Exp Cell Res. 2014 October 15; 328(1): 32–43. doi:10.1016/j.yexcr.2014.08.018.

Mitf regulates osteoclastogenesis by modulating NFATc1 activity

Ssu-Yi Lu,
Department of Diagnostic and Surgical Sciences, School of Dentistry, University of California, Los Angeles, CA, USA

Mengtao Li, and
Department of Diagnostic and Surgical Sciences, School of Dentistry, University of California, Los Angeles, CA, USA. CHS 23-087, 10833 Le Conte Ave., Los Angeles, CA 90095, USA

Yi-Ling Lin
Department of Diagnostic and Surgical Sciences, School of Dentistry, University of California, Los Angeles, CA, USA. Gene regulation program, Jonsson Comprehensive Cancer Center, University of California, Los Angeles, CA, USA

Ssu-Yi Lu: ssuyilu@yahoo.com.tw; Mengtao Li: mli@dentistry.ucla.edu

Abstract

Transcription factors Mitf and NFATc1 share many downstream targets that are critical for osteoclastogenesis. Since RANKL signals induce/activate both NFATc1 and Mitf isoform-E (Mitf-E), a tissue-restricted Mitf isoform in osteoclasts, it is plausible that the two factors work together to promote osteoclastogenesis. Although Mitf was shown to function upstream of NFATc1 previously, this study showed that expression of Mitf had little effects on NFATc1 and NFATc1 was critical for the induction of Mitf-E. In Mitf$^{mi/mi}$ mice, the semi-dominant mutation in *Mitf* gene leads to arrest of osteoclastogenesis in the early stages. However, when stimulated by RANKL, the Mitf$^{mi/mi}$ preosteoclasts responded with a significant induction of NFATc1, despite that the cells cannot differentiate into functional osteoclasts. In the absence of RANKL stimulation, very high levels of NFATc1 are required to drive osteoclast development. Our data indicate that Mitf functions downstream of NFATc1 in the RANKL pathway, and it plays an important role in amplifying NFATc1-dependent osteoclastogenic signals, which contributes to the significant synergy between the two factors during osteoclastogenesis. We propose that Mitf-E functions as a tissue-specific modulator for events downstream of NFATc1 activation during osteoclastogenesis.

†Corresponding author: Yi-Ling Lin. CHS 53-058B, 10833 Le Conte Ave., Los Angeles, CA 90095, USA. Tel: +13102064731; Fax: +13102064967. ylin@dentistry.ucla.edu.
Present address: Department of Biochemistry, Yong, Loo Lin School of Medicine, National University of Singapore, Block MD6, Centre for Translational Medicine, 14 Medical Drive, #14-01T, Singapore (117599)

Conflict of interest
The authors state no conflict of interest.

Keywords

Mitf; NFATc1; RANKL; transcription factors; fusion; osteoclasts

Introduction

During osteoclast differentiation, RANKL-RANK engagement activates multiple signaling pathways and a series of transcription factors including NF-κB, c-Fos, NFATc1 and Mitf [1–5]. Mutations of these genes result in arrest of osteoclast differentiation in various stages and the affected mice develop osteopetrosis. NFATc1 is regarded as the master transcription factor regulating osteoclast differentiation. Its induction and activation are the most critical events during osteoclastogenesis. Its master role is demonstrated by studies showing that NFATc1-deficient embryonic stem cells fail to differentiate into osteoclasts in response to RANKL stimulation and forced expression of a constitutively active form of NFATc1 (ca-NFATc1) leads to osteoclast differentiation from osteoclast precursors, bypassing the requirement of RANKL [3, 6]. Furthermore, expression of NFATc1 restores osteoclastogenesis in precursors derived from osteopetrotic NF-κB1/2 and c-Fos knockout (KO) mice [5, 7].

Among the transcription factors regulating osteoclastogenesis, Mitf is unique for its tissue-restricted effects, which have been suggested to be associated with the expressions of specific isoform (s) [8–17]. Mutations in *Mitf* gene profoundly affect only a few cell lineages, including osteoclasts, melanocytes, retinal pigmented epithelium and mast cells [18]. Mitf also plays roles in plasma cell differentiation and affects NK cell cytotoxicity [19–21]. A genome-wide screen of RANKL-inducible genes in bone marrow macrophages (BMM) showed that NFATc1 expression is significantly induced [6]. Although the screen did not find noteworthy changes of total Mitf expression, a later study examining the individual isoforms showed that Mitf-E levels are highly induced by RANKL stimulation during osteoclastogenesis [17]. Recently, transforming growth factor-β has been shown to enhance the effects of RANKL on Mitf-E expression [22]. Osteoclasts exhibit at least two major isoforms of Mitf, Mitf-A and Mitf-E. Unlike Mitf-E, expression of Mitf-A is ubiquitous and is abundantly present in both macrophages and osteoclasts. Mitf-A has a low osteoclastogenic activity, and RANKL stimulation does not result in significant induction as seen in Mitf-E [17], despite that it does fluctuate upon the stimulation.

Mitf and NFATc1 share many similar features. They have overlapping transcription targets [23–26], and both are critical for osteoclast fusion [27, 28]. In addition, Mitf-E and NFATc1 are significantly induced by RANKL signaling [6, 17, 29]. NFATc1 is widely expressed and is essential for the development of many tissues [30]. Although it is considered to be the master transcription factor for osteoclast differentiation [1], it is not clear how the ubiquitous NFATc1 can direct an osteoclast-specific transcriptional network. Given that Mitf-E has a restricted tissue distribution, we hypothesize that Mitf plays an important role in the NFATc1 signaling, mediating osteoclast-specific differentiation. In this study, we showed that Mitf-E fitted into the NFATc1 paradigm and functioned as an NFATc1 modulator during osteoclastogenesis.

Materials and Methods

Animal use

NFATc1 conditional KO mice were a gift from Dr. Antonios O. Aliprantis (Brigham and Women's Hospital, Boston, MA, USA). The mice were injected with polyinosinic-polycytidylic acid to ablate NFATc1 on day 10 after birth following the published protocol [26]. Wild type C57BL/6J mice were from UCLA DLAM Breeding Colony Services. Mice were euthanized by CO_2 inhalation. All procedures were performed in compliance with relevant laws and the usage has been approved by the Institutional Committee for Animal Care and Use Committee at UCLA.

Antibodies and chemicals

Antibodies were obtained from the following sources: α-myc (Cell Signaling, Inc., Beverly, MA. Catalog number: 2272), α-hemagglutinin (HA) (Roche Applied Science, Indianapolis, IN. Catalog number: 11867423001), α-NFATc1 (Santa Cruz Biotechnology, Inc., Santa Cruz, CA. Catalog number: sc-7294), α-Mitf (C5) (Calbiochem, San Diego, CA. Catalog number: MAB3747-I and a gift from Dr. David E. Fisher at Massachusetts General Hospital, Boston, MA) and α-tubulin (Sigma-Aldrich, St. Louis, MO. Catalog number: T9026-100UL). Cyclosporine A (CsA), polyinosinic-polycytidylic acid and SigmaFAST protease inhibitor were purchased from Sigma-Aldrich. Recombinant murine M-CSF and RANKL were purchased from PeproTech (Rocky Hill, NJ). All primers and probes were purchased from Integrated DNA technologies (Coralville, IA).

Plasmid constructs

The ca-NFATc1 fragment was first PCR-amplified from CA-NFAT2 plasmid [31] purchased from Addgene (Cambridge, MA), and then was subcloned to pCI-myc. pCI-myc was modified from pCI (Promega. Madison, WI) by inserting a myc tag sequence in front of the multiple cloning site. pMSCV-myc-ca-NFATc1 was generated by transferring the myc-ca-NFATc1 fragment to pMSCVpuro (Clontech, Mountain View, CA). Mitf fragments were derived from pcDNA-Mitf [17] and subcloned to pMSCVpuro and pMSCViG vectors. The pMSCViG vector has a HA tag sequence after the multiple cloning site. Primers and cloning details are summarized in Supplemental Table 1.

Cell cultures

Mice (ages 2–4 months) were euthanized by CO_2 inhalation. Femurs and tibias were dissected free of muscle, connective tissue and cartilage. The ends of the bones were clipped and cold media were used to flush the marrow out of the bone. An incision was made by scissors in the left back over the lower ribs and the peritoneal cavity was opened to expose spleen. Spleen was pulled out and cut away from fat, and then was mashed between the frosted ends of two glass slides to generate splenocyte suspension. Bone marrow and splenocytes were passed through 70 μm cell strainers to remove the tissue debris before plating. Bone marrow is a rich source of BMM. It was used for experiments in Figures 1, 3, 8 and all supplemental figures. Splenocytes were used in Figure 5C, as $Mitf^{mi/mi}$ mice are severely osteopetrotic and have little/no bone marrow. RAW264.7 cells (purchased from

ATCC), a murine preosteoclast cell line, were maintained in DMEM. All cell culture experiments were performed with MEM-α. To induce osteoclastogenesis, RAW264.7 cells and primary preosteoclasts (BMM and splenocytes) were supplemented with 50 ng/mL RANKL and 50 ng/mL RANKL plus 50 ng/mL M-CSF, respectively. RANKL treatment time is specified in the figure legends. For NFATc1 inhibition by CsA, cells were cultured with media containing CsA (2 μg/mL) for 30 minutes before adding RANKL, to assure complete inhibition. This process was repeated every time when media was changed. All cultures were supplemented with 10% FBS and standard antibiotics. Media in primary and RAW264.7 cultures were replenished every three days and two days, respectively. BAC1.2F5 cell line was cultured as described [32].

Retrovirus production

293FT cells (Invitrogen) were transfected with retroviral vectors together with pVPack-GP (Stratagene, La Jolla, CA) and pVSV-G (Clontech) using Lipofectamine 2000 (Invitrogen). Media of the transfected cells were collected 48–72 hours later and passed through 0.45 μm filters before spin-infecting the cells in the presence of 8 μg/mL polybrene at 1000g for 2 hours at room temperature.

RNA interference and lentivirus production

Lentiviral shRNAs targeting the mouse NFATc1 or Mitf sequence were purchased from Open Biosystems Products (Huntsville, AL, USA). Detailed information is provided in Supplemental Table 1. Scrambled shRNA in the same vector backbone pLKO.1 was purchased from Addgene. To produce lentiviruses, 293FT cells were transfected with a lentiviral vector, helper plasmid pCMV-DR8.9 and pVSV-G. Infection was conducted as described under “retroviral production”.

Real time quantitative polymerase chain reaction (RT-qPCR)

Total RNA was isolated with Trizol reagent (Invitrogen). 5 μg RNA was used in a reverse transcriptase reaction with an oligo-dT primer to generate cDNA using a SuperScript First-Strand Synthesis System (Invitrogen). RT-qPCR Taqman gene expression was performed on an Applied Biosystems 7500 Real-Time PCR system (Life Technologies) by using QuantiTech Probe PCR (Qiagen, Valencia, CA) according to the manufacturer’s instruction. Sequence-specific probes and primers were designed using a RealTime PCR software at IDT website http://www.idt.com. The relative standard curves of the targets were determined by dilution series of cDNA. mRNA levels were normalized to actin and expressed as relative values to those of the control cells (specified in the figure legends). Experiments were performed with at least two separate sets of samples and carried out in triplicate. Information of primers and probes is summarized in Supplemental Table 1.

Western blot

Cells were lysed in SDS/benzonase buffer (2% SDS, 50 mM Tris, pH 6.8, 10% glycerol, 0.1% benzonase and SigmaFAST protease inhibitor). Proteins were separated on SDS-polyacrylamide gels and transferred to nitrocellulose membranes. Membranes were blocked and incubated with the appropriate primary antibody followed by a HRP-conjugated

secondary antibody. The protein signal was developed with ECL reagent (Pierce Biotechnology, Rockford, IL, USA).

Tartrate resistant acid phosphatase (TRAP) stain

Cells were fixed and permeabilized with acetone/formalin/citric acid fixative followed by incubation with TRAP solution (Sigma-Aldrich, kit 387-A) at 37°C for 1 hour. For fluorescent TRAP staining, ELF97 was used as the phosphatase substrate [33].

Statistical analysis

All experiments were completed in triplicate and were repeated independently at least once. Data were analyzed using an unpaired two-tailed Student's *t*-test and were expressed as mean ± SD; $p \leq 0.01$ was considered significant.

Results

Induction of Mitf-E and NFATc1 by RANKL during osteoclast differentiation

RANKL plays an essential role for osteoclast differentiation and activation, and it is required throughout osteoclastogenesis. To differentiate preosteoclasts to multinucleated, bone resorbing osteoclasts *in vitro*, multiple treatments of RANKL were used to maintain the signal. Attached bone marrow cells, mostly BMM, were stimulated with RANKL over a 7-day time course to examine the temporal expression patterns of Mitf and NFATc1 (Fig. 1). Both NFATc1 and Mitf-E RNA levels were induced significantly in two days, which then declined sharply. The second treatment of RANKL on day 3 led to rebound of both transcription factors to the maximum levels in a day, followed by a slowly progressive and a swiftly sharp decline of NFATc1 and Mitf-E, respectively. RANKL stimulation on day 6 did not result in substantial induction of both factors. RNA levels of Mitf-A were not as closely associated with RANKL stimulation as those of Mitf-E and NFATc1. It went up moderately by first RANKL stimulation, roughly 3-fold, and the levels fluctuated within the range and showed no correlation with the subsequent stimulations throughout the course of osteoclast differentiation. Unlike Mitf-E, Mitf-A is normally present abundantly in osteoclast precursors and significant induction is not required for its cellular function. However, Mitf-A's osteoclastogenic activity is relatively weak and has been shown to be insufficient to fully support osteoclastogenesis [17].

Since bone marrow cells are not a homogenous population, RAW264.7 cells, a murine preosteoclast line, was used together with bone marrow cells to further investigate the relationship between RANKL, NFATc1 and Mitf.

Inhibition of NFATc1 diminishes induction of Mitf-E by RANKL

To determine the relationship between NFATc1 and Mitf-E, RNA interference by shRNAs was used to knock down the expression of NFATc1. Scrambled shRNA was used as control. Two NFATc1 shRNAs (N1 and N2) were introduced to preosteoclast RAW264.7 cells by lentiviral infection, and the cells were cultured in media containing RANKL to provide osteoclastogenic signals. Both shRNAs knocked down NFATc1. The N1 shRNA also specifically reduced the expression of Mitf-E but not that of Mitf-A (Fig. 2A). The N2

shRNA reduced expression of both Mitf isoforms, which raised the concern that the inhibition might be caused by off-target effects. BMM showed similar results (data not shown). The N1 was used for the subsequent western blot analysis. The results showed that NFATc1 knockdown greatly diminished the induction of RANKL-induced Mitf but had only mild effects on Mitf-A. (Fig. 2B, lane 4 vs. 2). We previously demonstrated that Mitf-E constitutes a significant portion of RANKL-induced Mitf [17]. Mitf appeared as multiple bands on the western blots. This is not only because different isoforms are generated by alternative promoter usage, but also because there are alternative splicing of the common exons. Protein phosphorylations also contribute to the complex band pattern. [2, 34–37].

To exclude the possibility that the above results were due to toxicity or global effects of RNA interference, NFATc1 inhibitor CsA was used. CsA inhibits calcineurin and prevents NFATc1 from undergoing dephosphorylation following RANKL signaling [38]. RAW264.7 cells were treated with RANKL twice for 3 days. RANKL were added on day 0 and day 2 in the presence or absence of CsA to better examine the effects of CsA on NFATc1 and Mitf-E induction by RANKL. This resulted in a robust induction and faster migration of NFATc1 protein seen in Figure 2C (lane 2) than those in Figure 2B (lane 2), as cells in Figure 2B received RANKL only once. The NFATc1 levels in cells not stimulated with RANKL also were less obvious due to shorter exposure of the western blot (Figs. 2C lane 1 vs. 2B lane 1). Figure 2C showed that the presence of CsA not only inactivated NFATc1, present as slower migrating bands, consistent with phosphorylated, inactive forms, but it also diminished the induction of RANKL-induced Mitf (lane 3 vs. 2). As mentioned, Mitf-E constitutes a significant portion of RANKL-induced Mitf.

We further examined if the above results were applicable to NFATc1 KO mice [26]. NFATc1 is the master transcription factor of osteoclasts; therefore, these mice do not develop osteoclasts. BMM derived from two age groups of NFATc1 KO and wild type (Wt) littermate mice were used for the study. RT-qPCR showed that NFATc1 KO BMM exhibited a significantly lower induction of Mitf-E by RANKL (Fig. 3A). Western blot showed diminished intensity of RANKL-induced Mitf (Fig. 3B). In contrast, Mitf-A expression was not consistently affected by the NFATc1 status.

These data establish the close relationship between NFATc1 and Mitf-E and indicate that NFATc1 expression is important for specific induction of Mitf-E by RANKL during osteoclastogenesis.

Constitutively active NFATc1 induces Mitf-E expression in the absence of RANKL stimulation

RANKL signaling induces and activates both NFATc1 and Mitf-E. Given the close relationship between the two factors, we next investigated if NFATc1 alone was sufficient to induce Mitf-E expression without the participation of other factors activated by RANKL. We took advantage of ca-NFATc1 [39], which is a constitutively active mutant of NFATc1. Ca-NFATc1 was introduced to RAW264.7 cells retrovirally to provide continuous NFATc1 signals in the absence of RANKL. Cells also were infected with retrovirus expressing green fluorescent protein (GFP). They were treated with or without RANKL, served as positive and negative controls, respectively. The results showed that, in the absence of RANKL, the

presence of ca-NFATc1 signals were sufficient to produce detectable Mitf-E signals in RAW264.7 cells (Fig. 4A). Western blot showed that overexpression of ca-NFATc1 induced additional Mitf bands, whose sizes were consistent with those of Mitf-E. Interestingly, ca-NFATc1 was also able to upregulate Mitf-A expression. The RT-qPCR showed that the presence of ca-NFATc1 without RANKL was able to induce Mitf-E expression to 22% of those in the positive control cells. (Fig. 4B). In BMM, ca-NFATc1 expression also induced Mitf-E expression from undetectable to detectable levels by RT-qPCR. However, the induction levels were significantly lower than those observed in RAW264.7 cells. It is only 31% of the Mitf-E levels detected in the positive control cells (Supplemental Fig. 1).

The observation that ca-NFATc1 alone is sufficient to induce Mitf-E expression without RANKL signaling, once again confirmed the critical role of NFATc1 in Mitf-E induction. Our data showed that there was no consistent association between Mitf-A levels and the NFATc1 activation induced by RANKL signaling, despite high levels of ca-NFATc1 were able to upregulate this isoform. We previously showed that Mitf-A has a lower osteoclastogenic activity and suggested that Mitf-E plays a critical role in mediating osteoclast differentiation [17].

Status of Mitf has no significant effects on NFATc1 expression

We also examined if Mitf status affected NFATc1. Mitf shRNA was introduced into osteoclast precursors by lentiviral infection to knockdown Mitf expression (Fig. 5A). Scrambled shRNA was used as control. Western blot showed that Mitf knockdown had only very mild negative effects on NFATc1 induction by RANKL. RT-qPCR confirmed the western blot results, and showed that even when Mitf levels were barely detectable by western blot (RNA levels ≈ 10% of the control); there still was a significant induction of NFATc1, roughly 73% of the control. Overexpression of Mitf-E also did not augment NFATc1 induction by RANKL (Fig. 5B). Unexpectedly, it actually led to lowered levels of NFATc1 in RAW264.7 cells. In BMM, the results of RNA interference were similar to those of RAW264.7, but overexpression of Mitf-E showed no effects on NFATc1 levels (Supplemental Fig. 2).

We further examined the role of Mitf in NFATc1 induction using $Mitf^{mi/mi}$ splenocytes as osteoclast precursors. The $Mitf^{mi/mi}$ mice have immature osteoclasts that cannot terminally differentiate into multinucleated, bone-resorbing osteoclasts, resulting in osteopetrosis [27, 28]. $Mitf^{mi}$ protein contains an arginine deletion in its basic domain and functions biochemically as a dominant negative. Therefore, it has broader inhibition ability, preventing all Mitf dimers, including homo- and hetero-dimers, from binding to their target promoters. Here, we investigated if impaired Mitf function affected NFATc1 levels in osteoclasts derived from $Mitf^{mi/mi}$ mice, and cells from wild-type littermate mice were used as control. As previously described [28], multinucleated giant cells were not observed in the $Mitf^{mi/mi}$ osteoclast cultures (Supplemental Fig. 3). However, these cells still responded to RANKL stimulation and exhibited a robust, despite slightly depressed, NFATc1 induction, estimated 80 % of the control value (wild-type mice) by RT-qPCR (Fig. 5C). Similar results were also obtained when mice with different age groups were assayed (data not shown). The

results indicated that Mitf did not play a significant role in RANKL-induced NFATc1 expression.

NFATc1 regulates vacuolar ATPase Vo domain d2 isoform (Atp6v0d2), which is a proton pump critical for osteoclast fusion [27, 28] [40]. Interestingly, despite the robust NFATc1 induction, $Mitf^{mi/mi}$ osteoclasts showed no upregulation of Atp6v0d2 following RANKL stimulation (Fig. 5C), indicating that NFATc1 required an active Mitf pathway to efficiently regulate its target Atp6v0d2. Taken together, these data suggest that Mitf functions downstream of NFATc1 during the RANKL signaling.

Overexpression of Mitf amplifies NFATc1-dependent osteoclastogenic signals

Mitf overexpression is sufficient to induce upregulation of many osteoclastogenic signals in RAW264.7 cells with or without RANKL treatment [17]. When overexpressing Mitf-E, RAW264.7 cells developed extensive cell-cell fusion and strong TRAP expression without RANKL treatment (Fig. 6A–C). However, these cells did not resorb bone and were smaller than mature osteoclasts (data not shown). Overexpression of Mitf-A only had minimal effects on the cells. This phenomenon not only was observed in RAW264.7 cells, but also was noted in macrophages BAC1.2F5 cells, which were not osteoclast precursor cells (data not shown). Expression of Mitf-E in RAW264.7 cells not treated with RANKL led to significant induction of important osteoclast genes Atp6v0d2, cathepsin K (Ctsk), dendritic cell-specific transmembrane protein (DC-STAMP) and TRAP (Fig. 6D). These genes also are regulated by NFATc1. Atp6v0d2 and DC-STAMP have been shown to be critical for cell-cell fusion in osteoclasts [40, 41].

Given the crucial role of NFATc1 signaling in osteoclast differentiation, it is necessary to know whether or not the Mitf-E action is associated with the NFATc1 pathway. Mitf-E-expressing RAW264.7 cells were treated with NFATc1 inhibitor CsA before stimulated by RANKL. The results showed that while the presence of 2 μg/mL CsA completely abrogated cell-cell fusion in the control GFP-expressing cells, ectopic expression of Mitf-E was able to overcome the NFATc1 inhibition and significantly promoted cell-cell fusion and strong TRAP expression (Fig. 7). The fusion phenomenon promoted by Mitf-E was abolished when NFATc1 was further inhibited by increasing CsA concentration to 10 μg/mL (data not shown), indicating that presence of NFAT activity was needed for the action of Mitf-E. Western blot in Figure 2C showed that cells stimulated by RANKL in the presence of 2 μg/mL of CsA still exhibited NFATc1 induction, but the protein bands were slower migrating, consistent with the phosphorylated bands, which indicated that this concentration of CsA strongly inhibited the activation of NFATc1. In BMM, however, overexpression of Mitf-E was insufficient to promote fusion in the absence of RANKL or when NFATc1 stimulation by RANKL was inhibited by CsA (Supplemental Fig 4).

The collaboration between NFATc1 and Mitf-E can be further demonstrated in studies with BMM derived from the NFATc1 KO mice. Osteoclasts derived from these mice exhibited less than 3% of NFATc1 mRNA and the protein was undetectable by western blot (Fig. 3). Overexpression of Mitf-E in these cells had a mild, but consistent, effect on promoting cell-cell fusion and TRAP expression. As shown in Figures 8A&B, Mitf-E expression did not result in extensive cell-cell fusion, and TRAP-positive cells that have more than 3 nuclei

were not found. Nonetheless, there was an increase of bi- or tri-nucleated TRAP-positive cells in the Mitf-E group (Fig. 8C). Expression of Mitf-E in NFATc1 KO cells treated with RANKL also significantly enhanced the expression of important osteoclast genes Atp6v0d2, Ctsk, DC-STAMP and TRAP (Fig. 8D). The induction of DC-STAMP by Mitf-E was very modest in the absence of NFATc1 (Figs. 6D and 8D). Strong expression of both ATP6v0d2 and DC-STAMP are required to generate large multinucleated osteoclasts.

The results indicated that expression of Mitf-E was able to promote certain osteoclast-related events even when the NFATc1 levels were low, indicating that the role of Mitf-E was involved in the amplification of the NFATc1 signaling during osteoclastogenesis. However, high levels of NFATc1 still are needed for cells to differentiate into full-sized, bone-resorbing osteoclasts.

Discussion

Mitf and NFATc1 have synergistic effects on osteoclastogenesis. It was shown that the Mitf-PU.1 complex is recruited to the target promoter before NFATc1 [23], and the synergy was attributed to their concomitant binding to the gene promoters that they co-regulate in osteoclasts. In this study, we showed that Mitf also functions downstream of NFATc1 during the RANKL signaling, and it can amplfy the NFATc1-dependent osteoclastogenic signals required to promote cell-cell fusion and strong TRAP expression. This provides an additional mechanism that is responsible for the synergistic effects between NFATc1 and Mitf.

Despite no effects on bone resorption, the presence of Mitf-E can lower the threshold requirement of NFATc1 for cell-cell fusion and TRAP expression. TRAP expression and multinuclearity are commonly associated, but not specific for, osteoclasts. ATP6v0d2 and DC-STAMP are essential for osteoclast fusion [40, 41]. Although Mitf has been shown to regulate DC-STAMP expression [42, 43], the RT-qPCR results indicated that Mitf's effects on DC-STAMP was very modest in the absence of sufficient levels of active NFATc1. Similarly, NFATc1 has been shown to regulate ATP6v0d2 [27], but the results from $Mitf^{mi/mi}$ cells indicated that NFATc1's upregulation had little effects on the levels of ATP6v0d2 in the absence of normal Mitf function. Therefore, insufficient DC-STAMP levels is likely the reason that cells with high Mitf-E and minimal NFATc1 levels, despite multinuclearity and TRAP expression, were smaller than mature osteoclasts. These cells failed to resorb bone, possibly also affected by the size.

Although NFATc1 is the master transcription factor of osteoclastogenesis, the event requires a network of transcription factors, including transcription repressors (reviewed by [44]). In *in vitro* osteoclastogenesis, NFATc1 and Mitf-E exhibited a close relationship during the first 4 days, and they went out of sync in later stages of development (Fig. 1). NFATc1 is critical for Mitf-E induction, but it can only partially induce Mitf-E, indicating that other transcription factors are required for the full induction. In the later stages of osteoclastogenesis, higher NFATc1 levels did not further augment the Mitf-E expression after day 4, suggesting that some negative mechanism may participate in the control of the Mitf-E expression at this stage.

In this study, primary osteoclast precursors and RAW264.7 cells were used, and the results were mostly comparible. However, discreipancies have been noted. In RAW264.7 cells, Mitf-E expression strongly promoted cell-cell fusion in the absence of RANKL and in the presence of RANKL when NFATc1 induction was inhibited by CsA. Nontheless, it showed little effects on promoting BMM fusion under similar culture conditions. The extent of Mitf-E induction by ca-NFATc1 were also different. It is plausible that RAW264.7 cells have some dysregulated signals that are not present in primary cells. These signals can coopoerate with Mitf-E and ca-NFATc1 to promote cell fusion and higher levels of Mitf-E induction, respectively. The process is not mediated by increased expression of NFATc1 (Fig. 5B). The putative signals in RAW264.7 cells may be related to NFAT, because very high levels of CsA (10 μg/mL) were able to completely inhibit cell fusion induced by Mitf-E (data not shown).

This study suggests that among NF-κB, c-Fos, NFATc1 and Mitf, four transcription factors that are activated during RANKL signaling, Mitf likely functions as the most distal factor. This notion is supported by the fact that the KO mice of the first three transcription factors do not develop osteoclasts while $Mitf^{mi/mi}$ mice develop immature osteoclasts [26, 28, 45, 46]. When cultured in osteoclastogenic media, NFATc1 KO BMM showed no osteoclast differentiation while $Mitf^{mi/mi}$ cells exhibited 1–3 nuclei with weak TRAP expression, consistent with immature osteoclasts (Supplemental Fig. 3).

We propose that Mitf-E is an NFATc1 signal modulator. NFATc1 is essential for the development of many tissues [30]. Although it is considered to be the master transcription factor for osteoclast differentiation [6], it is not clear how NFATc1 specifies an osteoclast-specific program from the other tissue differentiation programs that it also directs. It is plausible that osteoclast precursors control their differentiation program through collaboration of a “common” master transcription factor NFATc1 and a “tissue-restricted” transcription factor Mitf-E regulated by the master transcription factor. In this model, RANKL signaling initiates the osteoclast differentiation program by activating NFATc1, which leads to Mitf-E expression. Mitf-E has a restricted expression profile. Collaboration between Mitf-E and NFATc1 triggers osteoclast differentiation by turning on genes that are specifically associated with the features and functions of osteoclasts. This model also is supported by the data derived from the $Mitf^{mi/mi}$ osteoclast cultures (Fig. 5C). In these cells, there was still abundant active NFATc1 after RANKL stimulation, yet the NFATc1 target gene was not upregulated and significant fusion was abolished. The result indicates that Mitf signals are important for NFATc1-controlled osteoclast differentiation. Recently, a report showed that Mitf is critical for osteoclast lineage determination through a micro-RNA dependent mechanism [47].

In summary, Mitf-E appears to be a distal transcription factor in the RANKL signaling pathway. One of its roles is to positively modulate events downstream of NFATc1 activation during osteoclastogenesis.

Supplementary Material

Refer to Web version on PubMed Central for supplementary material.

Acknowledgments

We thank Drs. Jerold M. Schneider, John R. Basile for critical reading of the manuscript, Dr. David E. Fisher for the anti-Mitf antibody (C5), Dr. Antonios O. Aliprantis for the NFATc1 conditional KO mice and Dr. Richard Stanley for BAC1.2F5 cell line. This study was supported by National Institute of Dental and Craniofacial Research grant R03 DE019490 (to Y.L.L.).

Abbreviations

Atp6v0d2	vacuolar ATPase Vo domain d2 isoform
BMM	bone marrow macrophages
CsA	cyclosporin A
Ctsk	cathepsin K
DC-STAMP	dendritic cell-specific transmembrane protein
GFP	green fluorescent protein
HA	hemagglutinin
KO	knockout
Mitf	microphthalmia-associated transcription factor
Mitf-A	-E, Mitf isoform-A, -E
NFATc1	nuclear factor of activated T-cells, cytoplasmic 1
RANKL	receptor activator of nuclear factor kappa-B ligand
shRNA	short hairpin RNA
TRAP	tartrate resistant acid phosphatase
Wt	wild type

References

1. Asagiri M, Takayanagi H. The molecular understanding of osteoclast differentiation. Bone. 2007; 40(2):251–64. [PubMed: 17098490]
2. Mansky KC, et al. Microphthalmia transcription factor is a target of the p38 MAPK pathway in response to receptor activator of NF-kappa B ligand signaling. J Biol Chem. 2002; 277(13):11077–83. [PubMed: 11792706]
3. Hirotani H, et al. The calcineurin/nuclear factor of activated T cells signaling pathway regulates osteoclastogenesis in RAW264.7 cells. J Biol Chem. 2004; 279(14):13984–92. [PubMed: 14722106]
4. Gohda J, et al. RANK-mediated amplification of TRAF6 signaling leads to NFATc1 induction during osteoclastogenesis. Embo J. 2005; 24(4):790–9. [PubMed: 15678102]
5. Yamashita T, et al. NF-kappaB p50 and p52 regulate receptor activator of NF-kappaB ligand (RANKL) and tumor necrosis factor-induced osteoclast precursor differentiation by activating c-Fos and NFATc1. J Biol Chem. 2007; 282(25):18245–53. [PubMed: 17485464]
6. Takayanagi H, et al. Induction and activation of the transcription factor NFATc1 (NFAT2) integrate RANKL signaling in terminal differentiation of osteoclasts. Dev Cell. 2002; 3(6):889–901. [PubMed: 12479813]
7. Matsuo K, et al. Nuclear factor of activated T-cells (NFAT) rescues osteoclastogenesis in precursors lacking c-Fos. J Biol Chem. 2004; 279(25):26475–80. [PubMed: 15073183]

8. Hemesath TJ, et al. microphthalmia, a critical factor in melanocyte development, defines a discrete transcription factor family. Genes Dev. 1994; 8(22):2770–80. [PubMed: 7958932]
9. Hershey CL, Fisher DE. Genomic analysis of the Microphthalmia locus and identification of the MITF-J/Mitf-J isoform. Gene. 2005; 347(1):73–82. [PubMed: 15715979]
10. Amae S, et al. Identification of a novel isoform of microphthalmia-associated transcription factor that is enriched in retinal pigment epithelium. Biochem Biophys Res Commun. 1998; 247(3):710–5. [PubMed: 9647758]
11. Yasumoto K, et al. A big gene linked to small eyes encodes multiple Mitf isoforms: many promoters make light work. Pigment Cell Res. 1998; 11(6):329–36. [PubMed: 9870544]
12. King R, et al. Microphthalmia transcription factor. A sensitive and specific melanocyte marker for MelanomaDiagnosis. Am J Pathol. 1999; 155(3):731–8. [PubMed: 10487831]
13. Oboki K, et al. Isoforms of mi transcription factor preferentially expressed in cultured mast cells of mice. Biochem Biophys Res Commun. 2002; 290(4):1250–4. [PubMed: 11811997]
14. Takeda K, et al. Mitf-D, a newly identified isoform, expressed in the retinal pigment epithelium and monocyte-lineage cells affected by Mitf mutations. Biochim Biophys Acta. 2002; 1574(1):15–23. [PubMed: 11955610]
15. Takemoto CM, Yoon YJ, Fisher DE. The identification and functional characterization of a novel mast cell isoform of the microphthalmia-associated transcription factor. J Biol Chem. 2002; 277(33):30244–52. [PubMed: 12039954]
16. Shiohara M, et al. MITF-CM, a newly identified isoform of microphthalmia-associated transcription factor, is expressed in cultured mast cells. Int J Lab Hematol. 2008
17. Lu SY, Li M, Lin YL. Mitf Induction by RANKL Is Critical for Osteoclastogenesis. Mol Biol Cell. 2010; 21(10):1763–71. [PubMed: 20357005]
18. Steingrimsson E, et al. Molecular basis of mouse microphthalmia (mi) mutations helps explain their developmental and phenotypic consequences. Nat Genet. 1994; 8(3):256–63. [PubMed: 7874168]
19. Alinikula J, et al. Alternate pathways for Bcl6-mediated regulation of B cell to plasma cell differentiation. Eur J Immunol. 2011; 41(8):2404–13. [PubMed: 21674482]
20. Lin L, Gerth AJ, Peng SL. Active inhibition of plasma cell development in resting B cells by microphthalmia-associated transcription factor. J Exp Med. 2004; 200(1):115–22. [PubMed: 15226356]
21. Ito A, et al. Inhibitory effect on natural killer activity of microphthalmia transcription factor encoded by the mutant mi allele of mice. Blood. 2001; 97(7):2075–83. [PubMed: 11264174]
22. Asai K, Funaba M, Murakami M. Enhancement of RANKL-induced MITF-E expression and osteoclastogenesis by TGF-beta. Cell Biochem Funct. 2014; 32(5):401–9. [PubMed: 24519885]
23. Sharma SM, et al. MITF and PU.1 recruit p38 MAPK and NFATc1 to target genes during osteoclast differentiation. J Biol Chem. 2007; 282(21):15921–9. [PubMed: 17403683]
24. So H, et al. Microphthalmia transcription factor and PU.1 synergistically induce the leukocyte receptor osteoclast-associated receptor gene expression. J Biol Chem. 2003; 278(26):24209–16. [PubMed: 12695521]
25. Kim K, et al. Nuclear factor of activated T cells c1 induces osteoclast-associated receptor gene expression during tumor necrosis factor-related activation-induced cytokine-mediated osteoclastogenesis. J Biol Chem. 2005; 280(42):35209–16. [PubMed: 16109714]
26. Aliprantis AO, et al. NFATc1 in mice represses osteoprotegerin during osteoclastogenesis and dissociates systemic osteopenia from inflammation in cherubism. J Clin Invest. 2008; 118(11): 3775–89. [PubMed: 18846253]
27. Kim K, et al. NFATc1 induces osteoclast fusion via up-regulation of Atp6v0d2 and the dendritic cell-specific transmembrane protein (DC-STAMP). Mol Endocrinol. 2008; 22(1):176–85. [PubMed: 17885208]
28. Thesingh CW, Scherft JP. Fusion disability of embryonic osteoclast precursor cells and macrophages in the microphthalmic osteopetrotic mouse. Bone. 1985; 6(1):43–52. [PubMed: 3994857]
29. Asagiri M, et al. Autoamplification of NFATc1 expression determines its essential role in bone homeostasis. J Exp Med. 2005; 202(9):1261–9. [PubMed: 16275763]

30. Horsley V, Pavlath GK. NFAT: ubiquitous regulator of cell differentiation and adaptation. J Cell Biol. 2002; 156(5):771–4. [PubMed: 11877454]
31. Monticelli S, Rao A. NFAT1 and NFAT2 are positive regulators of IL-4 gene transcription. Eur J Immunol. 2002; 32(10):2971–8. [PubMed: 12355451]
32. Pollard JW, et al. Independently arising macrophage mutants dissociate growth factor-regulated survival and proliferation. Proc Natl Acad Sci U S A. 1991; 88(4):1474–8. [PubMed: 1996348]
33. Filgueira L. Fluorescence-based staining for tartrate-resistant acidic phosphatase (TRAP) in osteoclasts combined with other fluorescent dyes and protocols. J Histochem Cytochem. 2004; 52(3):411–4. [PubMed: 14966208]
34. Weilbaecher KN, et al. Linkage of M-CSF signaling to Mitf, TFE3, and the osteoclast defect in Mitf(mi/mi) mice. Mol Cell. 2001; 8(4):749–58. [PubMed: 11684011]
35. Bronisz A, et al. Microphthalmia-associated Transcription Factor Interactions with 14-3-3 Modulate Differentiation of Committed Myeloid Precursors. Mol Biol Cell. 2006; 17(9):3897–3906. [PubMed: 16822840]
36. Debbache J, et al. In vivo role of alternative splicing and serine phosphorylation of the microphthalmia-associated transcription factor. Genetics. 2012; 191(1):133–44. [PubMed: 22367038]
37. Hallsson JH, et al. Genomic, transcriptional and mutational analysis of the mouse microphthalmia locus. Genetics. 2000; 155(1):291–300. [PubMed: 10790403]
38. Li H, Rao A, Hogan PG. Interaction of calcineurin with substrates and targeting proteins. Trends Cell Biol. 2011; 21(2):91–103. [PubMed: 21115349]
39. Porter CM, Clipstone NA. Sustained NFAT signaling promotes a Th1-like pattern of gene expression in primary murine CD4+ T cells. J Immunol. 2002; 168(10):4936–45. [PubMed: 11994444]
40. Lee SH, et al. v-ATPase V0 subunit d2-deficient mice exhibit impaired osteoclast fusion and increased bone formation. Nat Med. 2006; 12(12):1403–9. [PubMed: 17128270]
41. Yagi M, et al. DC-STAMP is essential for cell-cell fusion in osteoclasts and foreign body giant cells. J Exp Med. 2005; 202(3):345–51. [PubMed: 16061724]
42. Choi J, et al. Caffeine enhances osteoclast differentiation and maturation through p38 MAP kinase/Mitf and DC-STAMP/CtsK and TRAP pathway. Cell Signal. 2013; 25(5):1222–7. [PubMed: 23434822]
43. Courtial N, et al. Tal1 regulates osteoclast differentiation through suppression of the master regulator of cell fusion DC-STAMP. FASEB J. 2012; 26(2):523–32. [PubMed: 21990371]
44. Takayanagi H. New developments in osteoimmunology. Nat Rev Rheumatol. 2012; 8(11):684–9. [PubMed: 23070645]
45. Iotsova V, et al. Osteopetrosis in mice lacking NF-kappaB1 and NF-kappaB2. Nat Med. 1997; 3(11):1285–9. [PubMed: 9359707]
46. Grigoriadis AE, et al. c-Fos: a key regulator of osteoclast-macrophage lineage determination and bone remodeling. Science. 1994; 266(5184):443–8. [PubMed: 7939685]
47. Mann M, et al. miRNA-based mechanism for the commitment of multipotent progenitors to a single cellular fate. Proc Natl Acad Sci U S A. 2010; 107(36):15804–9. [PubMed: 20720163]

Highlights

- Mitf functions downstream of NFATc1 in the RANKL pathway
- Mitf amplifies NFATc1-dependent osteoclastogenic signals
- Mitf-E functions as a tissue-specific modulator for NFATc1 signals during osteoclast differentiations

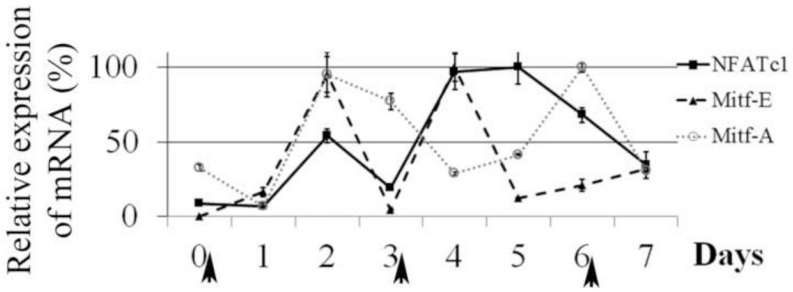

Fig. 1.

Temporal expression of Mitf-A, -E and NFATc1 in BMM during a 7-day time course of osteoclastogenesis by RT-qPCR. Media were replenished every 3 days to provide RANKL signals on days 0, 3 and 6 (indicated by arrows). The RNA levels measured on days 3 and 6 were performed without the scheduled media change. The maximum value of the mRNA during the time course was counted as 100%. The data were expressed as relative values.

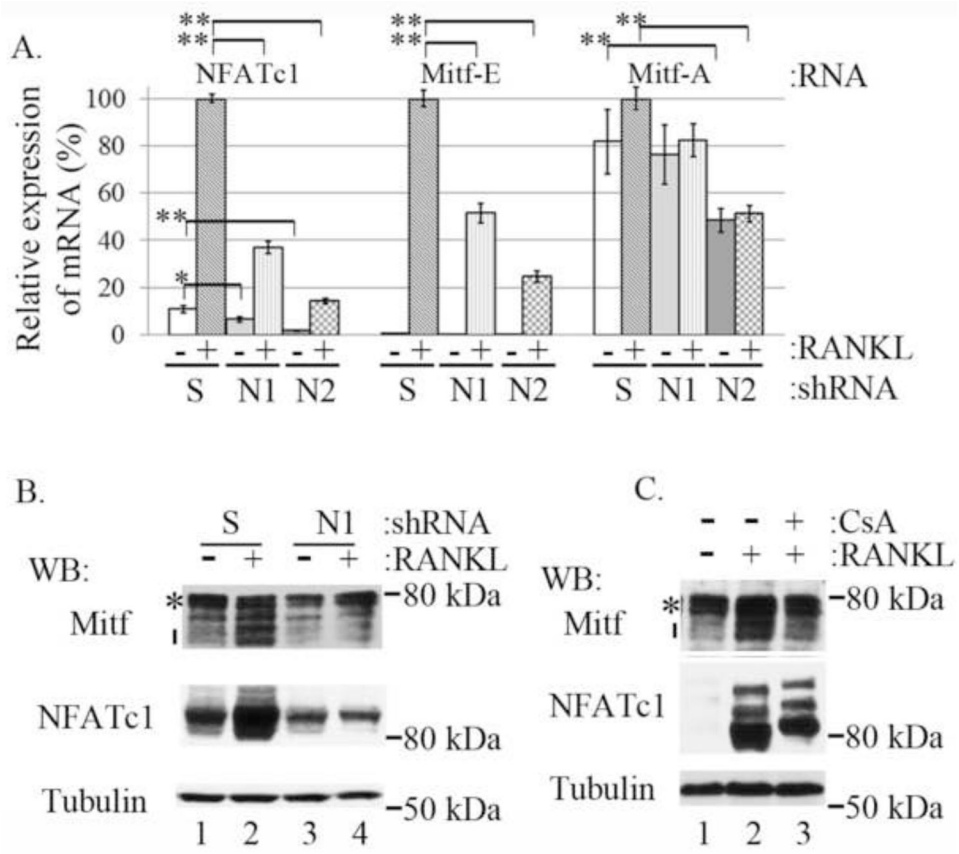

Fig. 2.

Mitf expression in NFATc1-knockdown RAW264.7 cells treated with RANKL. (A). RT-qPCR results of NFATc1, Mitf-E and Mitf-A expressions. Two different NFATc1 (N1 and N2) and a control scrambled (S) shRNAs were used. Cells were treated with or without RANKL for 2 days. The mRNA values of RANKL-stimulated control cells were counted as 100%. The data were expressed as relative values. *$p \leq 0.01$, **$p \leq 0.001$. (B). Western blot results of (A). Tubulin was a loading control. (C). Western blot results of cells treated with RANKL in the presence or absence of CsA for 3 days. Media were replenished on day 2. *: Mitf-A. ▮: RANKL-induced Mitf.

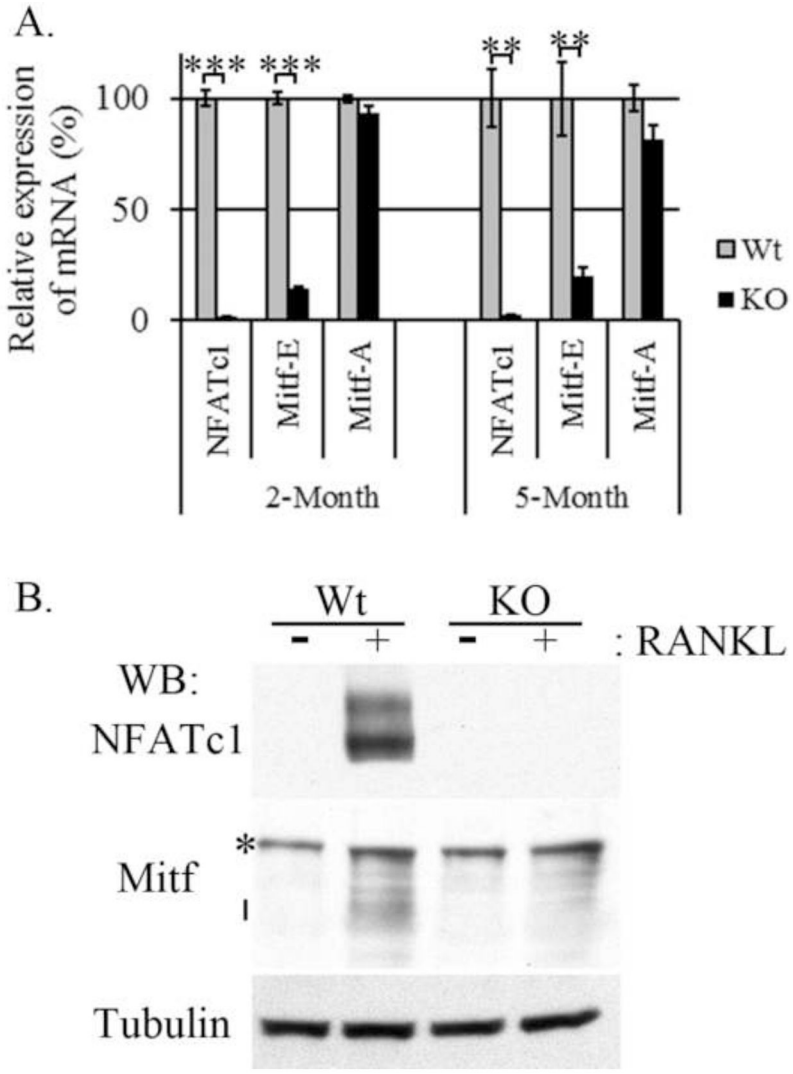

Fig. 3.

Mitf expression in NFATc1 KO BMM treated with RANKL. Cells were cultured with RANKL for 4 days. Media were replenished on day 3. Two age groups (2 and 5 months) were examined independently. Each group contained 3 pairs of NFATc1 KO and Wt littermate mice. (A). RT-qPCR results of NFATc1, Mitf-E and Mitf-A expressions. mRNAs were presented as relative values to those of the Wt cells. ** $p \leq 0.001$, *** $p \leq 0.0001$ (B). Western blot results of NFATc1 and Mitf. Tubulin was a loading control. *: Mitf-A. ▮: RANKL-induced Mitf.

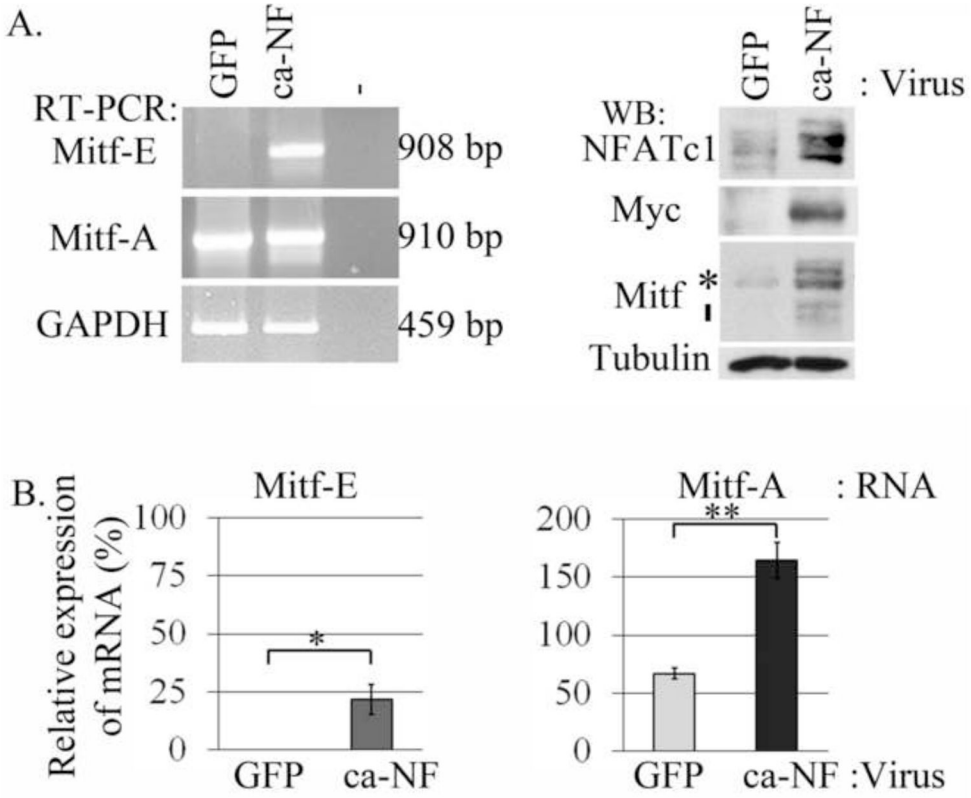

Fig. 4.

Effects of ca-NFATc1 on Mitf expression in RAW264.7 cells. Cells were infected with GFP or ca-NFATc1 (ca-NF) expressing retrovirus and cultured in media without RANKL for 2 days. (A). Left panel: Semi-quantitative PCR analysis of Mitf-A and -E. GAPDH was a loading control. -: No cDNA negative control. Right panel: Western blot analysis of NFATc1 and Mitf. Ca-NFATc1 was expressed as a myc-tagged protein. *: Mitf-A. ▮: ca-NFATc1-induced Mitf. (B). RT-qPCR quantitation of Mitf-E and -A. mRNAs were presented as relative values to those of GFP expressing cells treated with RANKL. *$p \leq 0.01$ **$p \leq 0.001$.

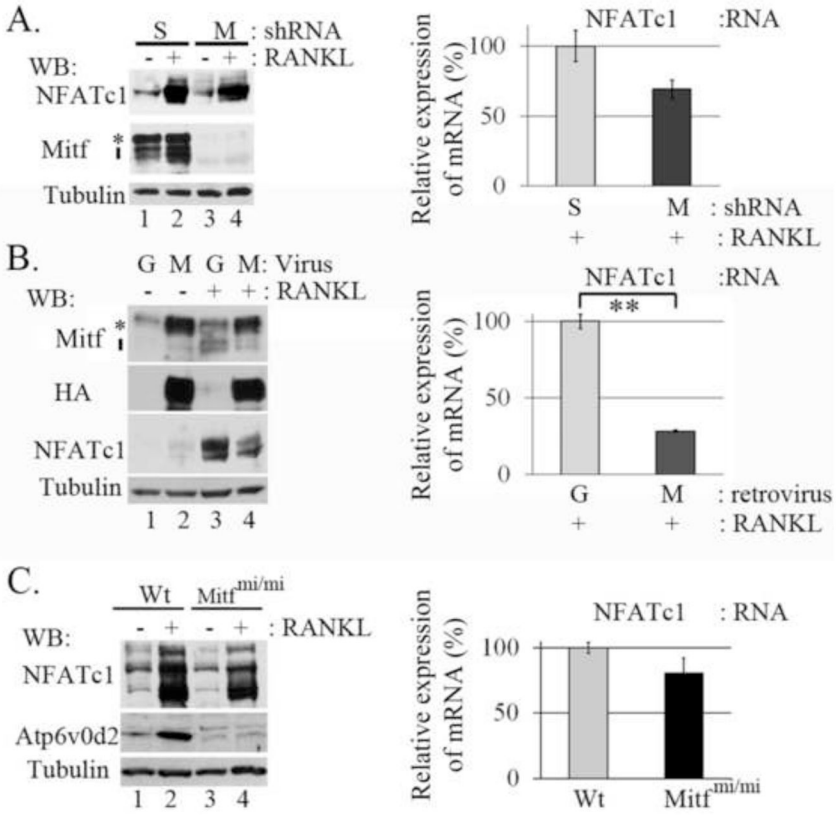

Fig. 5.

Effects of Mitf status on NFATc1 expression in RANKL-treated preosteoclasts. (A). Effects of Mitf inhibition on NFATc1 induction by RANKL. Western blot and RT-qPCR analyses of RAW264.7 cells infected with scrambled (S) or Mitf (M) shRNA lentivirus. The cells were cultured in media supplemented with or without RANKL for 2 days. *: Mitf-A. ❙: RANKL-induced Mitf. (B). Effects of Mitf-E overexpression on NFATc1 induction by RANKL. Western blot and RT-qPCR analyses of RAW264.7 cells infected with GFP (G) or Mitf-E (M) expressing retrovirus. The cells were cultured in media with or without RANKL for 2 days. The recombinant Mitf-E had a HA tag and the resulting fusion protein migrated with a similar electrophoretic mobility to the endogenous Mitf-A. *: Mitf-A and Mitf-E-HA (recombinant). ❙: RANKL-induced Mitf. ** $p \leq 0.001$. (C). Western blots and RT-qPCR of splenocyte cultures derived from $Mitf^{mi/mi}$ and wild type (Wt) littermate mice. Cells were treated with or without RANKL for 4 days. Media were replenished on day 3.

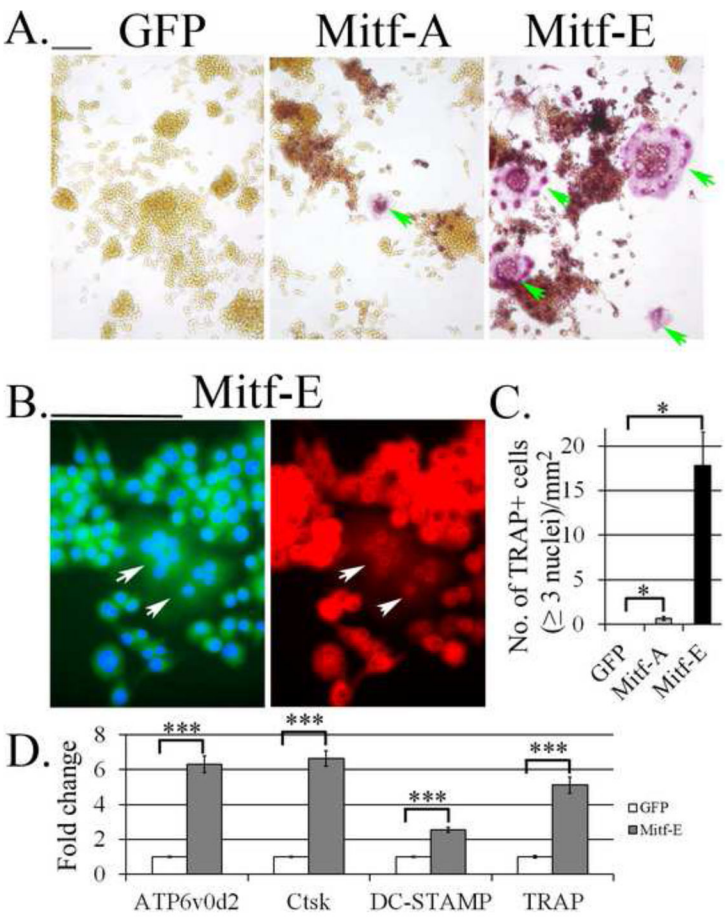

Fig. 6.

Effects of ectopic expression of Mitf-A and -E on TRAP expression and cell fusion in RAW264.7 without RANKL. GFP, Mitf-A or Mitf-E was introduced to RAW264.7 cells retrovirally. (A) TRAP stain. Multinucleated cells (shown by arrows). (B). Multinuclearity (shown by arrows) of Mitf-E expressing cells in (A). Mitf-E-HA expression was detected with α-HA Ab by immunofluorescent staining (red). Cells were counterstained with DAPI, which stains the nuclei (blue). An IRES-GFP sequence was present in the viral vector, which resulted in GFP expression in the infected cells (green). Horizontal bar: 100 μm. (C). Number of TRAP + cells that have ≥ 3 nuclei per mm^2 in (A). (D). RT-qPCR quantitation of ATP6v0d2, Ctsk, DC-STAMP and TRAP in Mitf-E expressing RAW264.7 cells in (A). mRNAs were presented as fold induction relative to those of GFP expressing cells without RANKL. *$p \leq 0.01$ ***$p \leq 0.0001$.

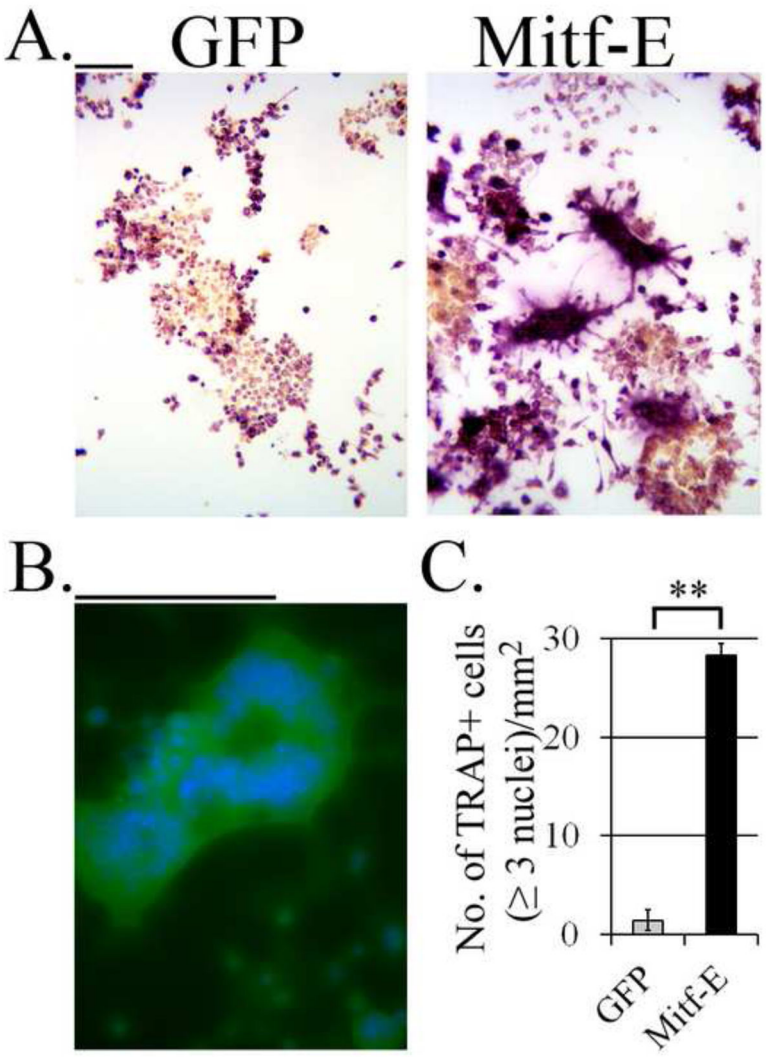

Fig. 7.

Effects of ectopic expression of Mitf-E on TRAP expression and cell fusion in RAW264.7 cells when NFATc1 is inhibited by CsA. GFP and Mitf-E were introduced to RAW264.7 cells retrovirally. The infected cells were treated with CsA before being cultured in the presence of RANKL. (A). TRAP stain. (B). Multinuclearity of Mitf-E expressing cells in (A). DAPI stains the nuclei (blue). (C). Number of TRAP + cells that have ≥ 3 nuclei per mm^2 in (A). $^{**}p \leq 0.001$. Horizontal bar: 100 μm.

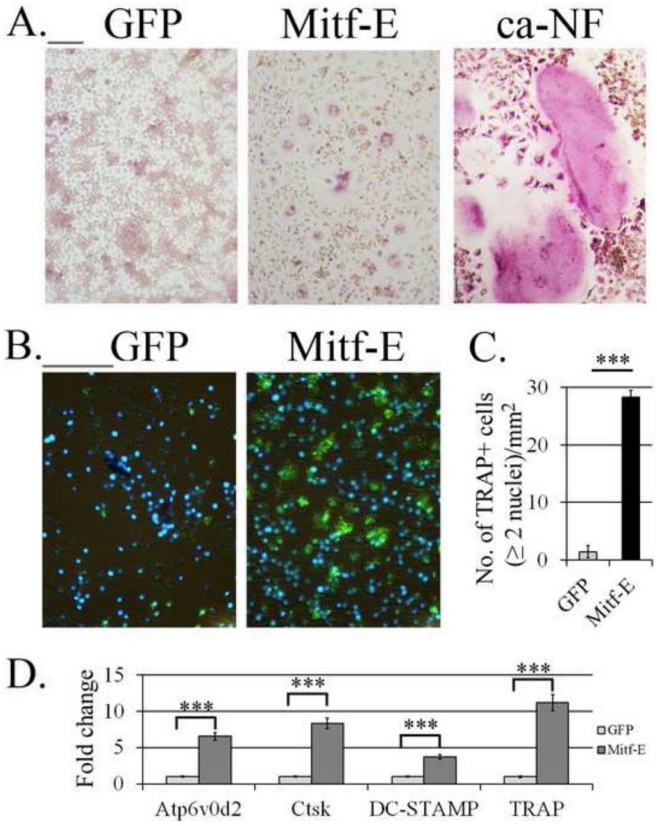

Fig. 8.

Effects of ectopic expression of Mitf-E on TRAP expression and cell fusion in NFATc1 KO BMM cultured in osteoclastogenic media. GFP, Mitf-E or ca-NFATc1 (ca-NF) was introduced to BMM retrovirally. Ca-NFATc1 was a positive control. (A) Colored TRAP stain. (B). Fluorescent TRAP stain. Green: TRAP. Blue: DAPI, stains nuclei. (C). Number of TRAP + cells that have ≥ 2 nuclei per mm^2 in (A). ***$p \leq 0.0001$. (D). RT-qPCR quantitation of ATP6v0d2, Ctsk, DC-STAMP and TRAP in Mitf-E expressing NFATc1 KO BMM cultured in osteoclast differentiation media. Horizontal bar: 100 μm.